Journal of Non-Crystalline Solids: X 18 (2023) 100191

Contents lists available at ScienceDirect

Journal of Non-Crystalline Solids: X

journal homepage: www.sciencedirect.com/journal/journal-of-non-crystalline-solids-x

Molecular simulations of the strength enhancement of pre-stressed silica glass upon exposure to moisture

Stephen H. Garofalini

Interfacial Molecular Science Laboratory, Department of Materials Science and Engineering, Rutgers University, USA

ARTICLE INFO

Keywords:
Silica
Water
Fracture
Silanols
Pre-stressing

ABSTRACT

Molecular dynamics simulations were used to evaluate the fracture strength of pre-stressed silica glass exposed to water molecules, with and without heating. The pre-stressed wet glasses had a strength enhancement of 5–7% in comparison to the original dry glasses. Heating the glasses while pre-stressed with included water resulted in an even greater strength enhancement. The glasses with a higher concentration of structural defects in the dry glass have an expected lower dry-glass strength in comparison to the glass with fewer defects. However, the weaker dry glass shows a greater strength enhancement after pre-stressed water exposure caused by the increase in the silanol concentration in the more defective glass that offsets the otherwise weakened glass. Increased silanol concentration has been shown to increase the expansion of silica glass, creating an increased compressive stress on the pre-stressed-wet glass relaxed to original dimensions, allowing for an increased strength enhancement.

1. Introduction

Studies by Tomozawa and colleagues have shown that water at a specifically prepared amorphous silica (a-SiO_2) surface can be used to strengthen the glass [1–9]. This is clearly in contrast to the well-known weakening of silica exposed to water while under tension in stress corrosion cracking, so the implication of Tomozawa's work is significant.

The interactions between water molecules and the silica surface have been well characterized in experimental and computational studies [10–33]. The rupture of strained siloxane (Si-O-Si) bonds by water molecules enables crack propagation via the model originally proposed by Michalske and Freiman [12,13]. Subsequent studies showed the significantly higher reactivity in the 2- and 3-membered rings in silica in comparison to the average ring sizes (5–6 membered rings) [11] and such small rings are known to exist at the outer silica surface upon fracture in a dry environment. [14]

However, Lezzi et al. showed that by straining a silica fiber below its fracture strength while simultaneously exposing the fiber to water vapor at an elevated temperature followed by relaxation of the stress created a surface in compression [3,4]. Similar to glass strengthening mechanisms involving ion-exchange, a glass surface in compression increases the fracture strength of the glass. The strength increase is related to the amount of induced strain during water absorption [3,8]. There is also a relation between the concentration of absorbed water, volume expansion, and strength enhancement [34].The strengthening mechanism observed by Tomozawa's group has also been observed in studies by Wiederhorn and colleagues [9,34–37].

An associated issue related to the strength enhancement is the affect of absorbed water on volume expansion of silica [38,39]. The cause of this expansion has been attributed to either of two separate mechanisms: one, the expansion is caused by molecular water in the glass [1–8]; or two, the expansion is caused by silanol (SiOH) groups [9,34–37]. Molecular simulations by Garofalini's group showed that silanols and not intact water molecules caused the observed expansion, supporting the silanol-driven mechanism [31].

In the molecular dynamics simulations presented here, silica glasses were prepared as dry glasses and as glasses that have water introduced in strained glasses in a manner that generally mimics the protocols presented by Tomozawa (expanded, water introduced, relaxed to original size, strained to fracture to determine strength).

In order to allow for reactions between the water and the silica glass in the molecular dynamics simulations, we use a reactive all-atom potential with two- and three-body terms. [27,40] A variety of bulk water properties have been observed using this potential, such as the O—O pair distribution function, heat of vaporization (10.5 kcal/mol), diffusion coefficient (2.4×10^{-5} cm^2/s), and frequency spectrum [27,40]. Consistent with experimental data, hydrogen bond lifetimes in bulk water are 2.1 ps. [41] Proton transport in bulk water via the Grotthuss mechanism is observed in simulations of water [41,42] with a free

E-mail address: shg@rutgers.edu.

https://doi.org/10.1016/j.nocx.2023.100191
Received 20 March 2023; Received in revised form 6 June 2023; Accepted 7 June 2023
Available online 12 June 2023

energy barrier of proton transter at 2.4 Å O—O spacing within 0.2 kcal/mol of the ab-initio calculations [42,43]. The large jump angular correlation function of hydrogen bond motion is also consistent with experiment [41]. Simulations of the frequency-frequency correlation function in bulk water showed short-time correlations similar to experiment and long-time behavior that coincides with the O—O vibrations [44]. Silica surfaces exposed to water form surface silanols (SiOHs) at concentrations (4–5 nm^{-2}) consistent with experiment [45]. Proton migration at the silica surface via surface silanols and adjacent waters, forming H_3O^+ ions [21,27,45], is consistent with ab-initio calculations [18]. Application to nanoconfined water in silica showed the high thermal expansion observed experimentally [20,23].

Using this robust and transferrable potential, the resultant strengths of the dry versus wet glasses are simulated and compared. Details of the protocol are given in the computational procedure. The result of the simulations shows that with an ~5% strain in one dimension and 5 wt% water put into the expanded glass, followed by return to the original dimension, a strength increase of ~5% is observed in the simulations. This is consistent with the observations by Lezzi et al [3]

2. Computational procedure

The reactive multibody force field [27,31,40–42] discussed above is used in the current simulations. A silica glass containing 3888 SiO_2 units (11,664 atoms) was produced in 2 separate base melt/quench procedures, with protocols for making additional glasses. In the melt/quench process and any elevated temperature runs, the experimental coefficient of thermal expansion (CTE) of silica was used for the volume change at each temperature in all runs, which allowed for greater mobility of the atoms at the high temperatures. However, since the glass transition temperature for silica glass using this potential is near 2200 K, the contraction at and below 2000 K would be reasonable. Glass A* went through the melt/quench procedure of 6000 K for 100,000 timesteps, 5000 K for 500,000 timesteps, and 4000 K, 3000 K, 2000 K, 1800 K, 1500 K, 1000 K, and 300 K each for 1,000,000 timesteps for a total of 7.6×10^6 timesteps and was used to generate other glasses. A timestep of 1 fs was used in this constant number, volume and temperature (NVT) process. Glass A* dimensions at 298 K were 63.587 Å, 63.761 Å, and 43.471 Å in x, y, and z, respectively. Glass B was made starting from the end of the Glass A* quench in an additional order of magnitude slower melt/quench: 6000 K for 500,000 timesteps, and 5000 K, 4000 K, 3000 K, 2000 K, 1800 K, 1500 K, 1000 K, and 300 K each for 10,000,000 timesteps for a total of 85×10^6 timesteps. Following this, an additional NPT (constant number, pressure, temperature) was run at 298 K for 100,000 timesteps for Glass B. Glass B has average dimensions of 63.319 Å, 63.677 Å, and 43.499 Å in x, y, and z, respectively. Glasses A* and B had densities of 2.20 and 2.21 g/cc, respectively. Glass A* was also made into 3 additional bulk glasses, called A1, A2, A3, that have relatively large defect concentrations (compared to glass B that has fewer defects, as discussed below).

Each glass was strained 5% in the x dimension and 5 wt% water was then added, followed by shrinkage to the original dimension and subsequent calculation of the stress/strain curves, as presented below.

Glasses were evaluated in dry and wet scenarios as depicted in Fig. 1. In Scenario 1, glasses A1–3 and B were evaluated as bulk systems (3-dimension periodic boundary conditions (PBC)); in Scenario 2, pre-stressed wet glasses were heated to 700 K for 200,000 timesteps to increase the concentration of SiOH's and reduce the concentration of intact H_2O molecules via water/silica reactions. The glasses were then cooled to 298 K and run for 200,000 timesteps, then returned back to the original dimension that existed prior to the 5% strain. Since it has been shown that increased SiOH concentration causes increased volume expansion in silica [9,31,34–37], such a result might be expected to cause an increase in the effective compression of the expanded glass upon return to its original x dimension prior to the final stress/strain to fracture. Note, the experimental work had incorporated water into the expanded glass fibers using elevated temperatures prior to release of the stress. Lezzi et al. observed a strength increase nearly equal to the imposed tensile stress during exposure to water [3].

In addition to obtaining the stress/strain curves for the dry glasses taken at step 1 in Fig. 1, Fig. 1 shows a schematic of the processes involving the wet and wet/heated systems. Fig. 1 shows the dry bulk

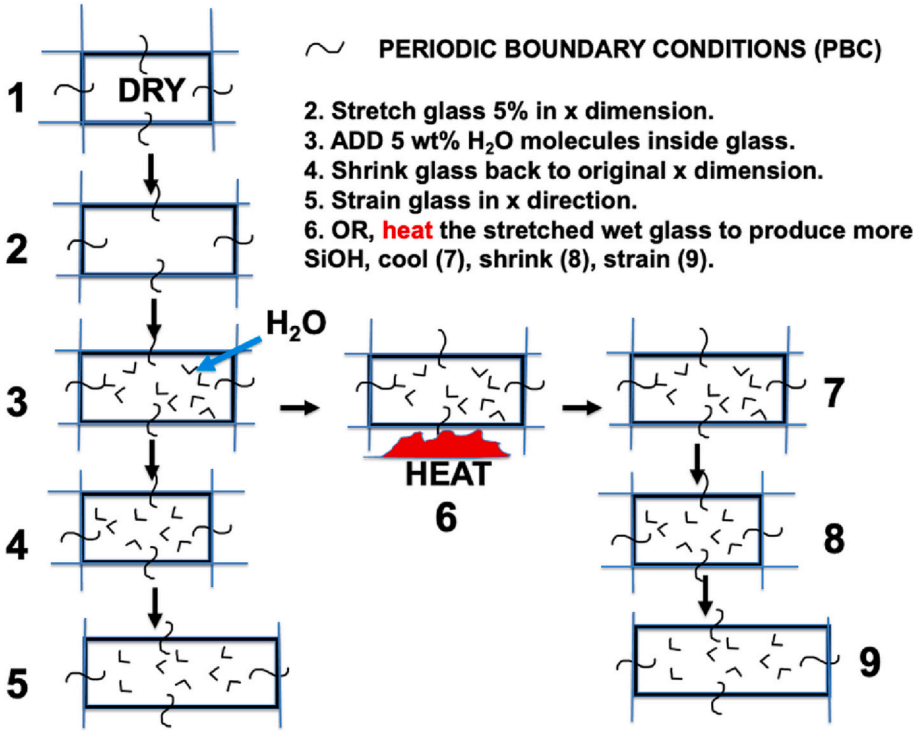

Fig. 1. Schematic of the process used to make the bulk glass with 5 wt% water and heating. See text for details of the numbered steps.

glass at step 1 that is stretched 5% in the x dimension at step 2 using the same strain rate that was used later for determination of the stress/strain curves. At step 3, 5 wt% water was randomly added to each stretched glass in a manner presented below, then the wet glass was reversed strained (compressed) the appropriate amount to bring the glass back to the original x dimension at step 4, then strained to failure at step 5 to obtain the stress/strain curve. In addition, considering step 3, the wet expanded glass was also heated to 700 K at step 6, then quenched to 298 K at step 7, returned to its original x dimension at step 8 by reversing the strain an appropriate amount, and then strained to failure at step 9. The 5% expansion of the dry glasses in the x dimension in step 2 resulted in a tensile stresses from ~5.4 GPa to 6.0 GPa for glasses A1–3 and B. Given the results by Lezzi et al., we might expect a strength increase near these values for the glasses at steps 5 or 9 in Fig. 1.

Glass A* was shifted up 15 Å in the z direction and the PBC in the z dimension was simultaneously removed to create a glass film with 2 free surfaces. Bulk glass A1 was formed from this dry film version of A* by shifting the atoms back 15 Å in z and simultaneously including the PBC in the z dimension. Since surface relaxation had occurred, this created a few species that were close to each other and caused significant repulsion forces that caused some atoms to become ballistic in the glass. While unconventional, this process allowed for significant defect formation, as presented below in Table 1. Bulk glass A2 was formed from A1 as A1 was relaxed at 1000 K for 200,000 timesteps followed by a quench to 298 K and run for another 100,000 timesteps, reducing the defect concentrations. Finally, bulk glass A3 was made from bulk glass A* in NPT simulations using constant 1 atm pressure in x and y dimensions and running for 100,000 timesteps at 2000 K then 100,000 timesteps at 298 K. This reduced the defects further, also shown in Table 1.

In all stretched glasses, the systems had different sets of water molecules added at a constant concentration of 5 wt% using the Park-Miller random number generator with the Bays-Durham shuffle [46,47]; different random number initiators were used for water insertion in each glass so that the inserted water had different starting locations in each glass. This constant number of water molecules (650) was inserted within each glass while in the expanded state (5% expansion) using a minimum separation distance of 2.7 Å to any O or Si atoms existing in the system at the time of insertion (including previously inserted water molecules). As mentioned above, each of the wet expanded glasses was eventually reverse-strained back to their original x dimension. The timestep for all simulations involving just silica in the melt/quench process was 1×10^{-15} s. The timestep for all simulations involving water was 1×10^{-16} s due to the presence of the protons. For consistency, the timestep used in generating the stress/strain curves was also 1×10^{-16} s, regardless of whether water was present or not. In all simulations involving straining the samples, the strain rate was 4×10^{-3} ps^{-1}. The x position of each atom was incrementally strained as a function of its x position every 100th timestep. The stress was calculated by the standard stress tensor previously presented [48,49]. Of course, the simulations might mimic, but not specifically reproduce, the experimental procedure for obvious reasons.

Table 1
Number of 3-coordinated Si (3-CN Si), non-bridging oxygens (NBO), and 3 coordinated oxygens (3-CN O) in dry glasses A1–3 and B showing the decreased defects in going from glass A1, A2, A3, and B. Percent of defects relative to the concentration of Si or O in the silica also shown. There were no 5-coordinated Si in any glass. The Si—O cutoff distance was 2.0 Å for determination of coordination.

GLASS	3-CN Si	NBO	3-CN O
A1	92 (2.4%)	121 (1.6%)	49 (0.63%)
A2	69 (1.8%)	106 (1.4%)	38 (0.49%)
A3	25 (0.64%)	52 (0.67%)	27 (0.35%)
B	11 (0.28%)	33 (0.42%)	22 (0.28%)

3. Results and discussion

Examples of the results of the stress/strain calculations are shown in Fig. 2 for the glasses fractured at step 1 in Fig. 1 (called DRY in Fig. 2) and with 5 wt% water included and fractured in step 5 in Fig. 1 (called WET in Fig. 2) for the glass with the highest number of defects in the dry glass (A1) in comparison to glasses with fewer initial defects (A2 and A3 in 2a and B in 2b), showing a distinct difference in the dry glass strengths. The figure also shows the increase in strength maximum for each wet glass containing 5 wt% water added to the 5% strained and subsequently relaxed glass in comparison to its dry glass version. The wet and wet-heated glasses experienced the expected compressive state after return to the original x dimension. The initial negative (compressive) stresses during the fracture calculations were − 0.32 GPa for A1, −0.31GPa for A2, −0.29 GPa for A3 and − 0.09 GPa for B. The stress curves were shifted up by the absolute values of these stresses to have a zero stress start for comparison to the dry glasses.

Fig. 3 provides the increase in stress relative to the maximum stress in dry glass A2 in (a) and the maximum in dry glass B in (b). Also included in the figures is the result of heating each stretched glass with water included (step 6 in Fig. 1 and labeled HEAT in Fig. 3) showing an even greater strength increase. The increase in strength is related to the imposed tensile stress in step 2 in Fig. 1 and the resultant compressive stress in the glasses at steps 4 and 8. The specific data are presented in Table 2 for the maximum stress at failure and the percent increase from the dry-glass value. As shown below, these different stresses are related

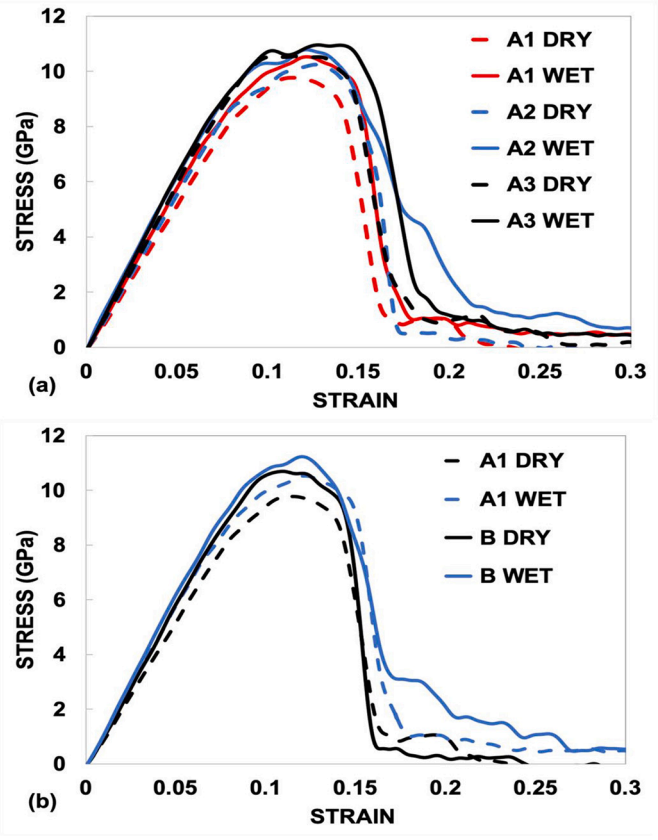

Fig. 2. (a) Stress/strain results for the A1–3 bulk glasses with (WET) and without (DRY) 5 wt% water. Dashed lines are for the dry glasses and solid lines are for the wet glasses. (b) Dashed lines for glasses A1 dry and wet and solid lines are glass B. In both (a) and (b) results show increased strengths for the wet glasses in comparison to the dry glasses and increased strength for glasses with fewer initial defects (A1 to A3 in (a) and A1 to B in (b)). Wet glass curves are shifted to zero stress at zero strain to account for the initial compressive stress caused by the water insertion.

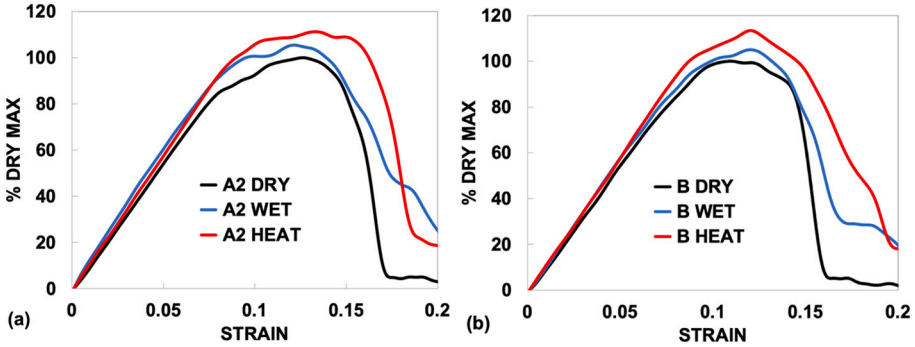

Fig. 3. Stress/strain curves for glass A2 (a) and glass B (b) relative to the maximum stress observed in the dry glass for each. The 'HEAT' indicates step 6 in Fig. 1.

Table 2
Maximum stress at failure and the increase from the dry glass value for glasses A1–3 and B, wet and wet plus heat treatment, as per Fig. 1.

GLASS	Stress Max (GPa)			Increase %	
	DRY	WET	HEAT	WET	HEAT
A1	9.77	10.52	11.50	7.6	17.7
A2	10.23	10.79	11.37	5.5	11.1
A3	10.55	10.95	11.77	3.8	11.6
B	10.69	11.23	12.13	5.0	13.4

to the concentration of silanols in these two glasses at the start of the subsequent calculations of fracture strength.

These simulation results are similar to the experimental results obtained by Lezzi [3]. Also, in Lezzi et al., the glass under an applied tensile stress was exposed to water at an elevated temperature (to enable water penetration) followed by removal of the applied stress with the glass returning to its original dimension, whereupon the glass was strained to failure. Fig. 3 and Table 2 show that the inclusion of elevated temperature results in an even greater increase in the glass strength in comparison to the glasses that were strained to failure without pre-heating.

The structure of the glasses can be observed in the pair distribution functions (PDFs), as shown in Fig. 4. Glass A2 has more defects than glass B caused by the melt/quench procedures for making the glasses. Step 4 in Fig. 1 (wet-strained glass returned to original x dimension) resulted in different concentrations of defect species in the glasses (3-coordinated Si, NBO's, and 3-coordinate O) as listed in Table 1. These defects are present at the start of the subsequent stress/strain calculations to fracture. These different initial structures have an impact on the concentrations of silanols (SiOH's) that form in the glasses and the concomitant decrease in the concentrations of remaining (unreacted) water molecules, as shown in Fig. 5.

Fig. 5 shows the concentrations of intact H_2O molecules and SiOH species relative to the original 5 wt% H_2O added for bulk glasses A2 and B as a function of strain during the simulations used to obtain the fracture strength. The data shown in Fig. 5 takes these values to the strain that is at the stress maximum in each glass seen in Figs. 2 and 3. Glass B had a much slower melt/quench process than glass A2 and shows far fewer SiOH at the beginning of the tensile fracture run. In each case, the initial data point would be indicative of the concentration of silanols present near the start of the stress/strain runs. Nonetheless, the characteristics are the same for each wet glass: the shapes of the curves are similar for the specific species shown and each curve shows a significant change in slope near 9–10% strain. This rapid increase in the concentration of SiOH's at this strain is similar to the change in slope in the stress/strain curve in Figs. 2 and 3 as the maximum stresses are approached. As the strain is increased, strained siloxane bonds are ruptured by reactions with the water molecules and the concentration of silanols increases rapidly and the stress maximizes.

Fig. 5 also includes the percent concentrations of these species after the heat treatment during water insertion at step 6 (labeled HT). The inclusion of heating after insertion of the water into the glasses shows the expected increased reactions forming a loss of intact water molecules (filled red circles and squares) as compared to the glasses that did not have this additional heat treatment (filled black circles and squares), with the expected increase in the silanols (open red circles and squares). Interestingly, the elevated temperature created the increase in silanols

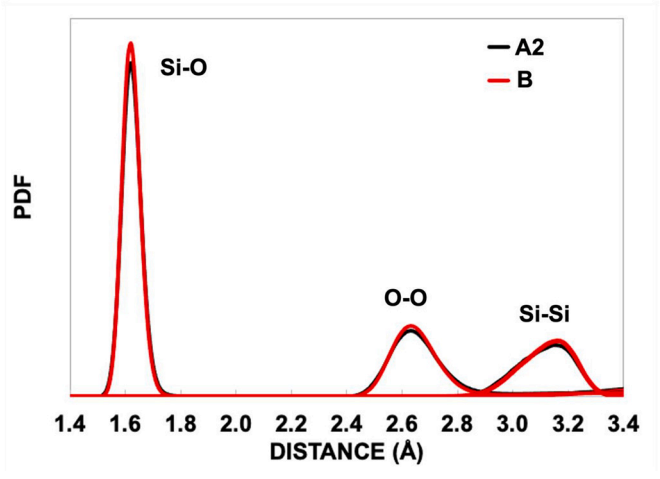

Fig. 4. Pair distribution functions of the 2 dry bulk glasses showing a difference between glass A2 and glass B.

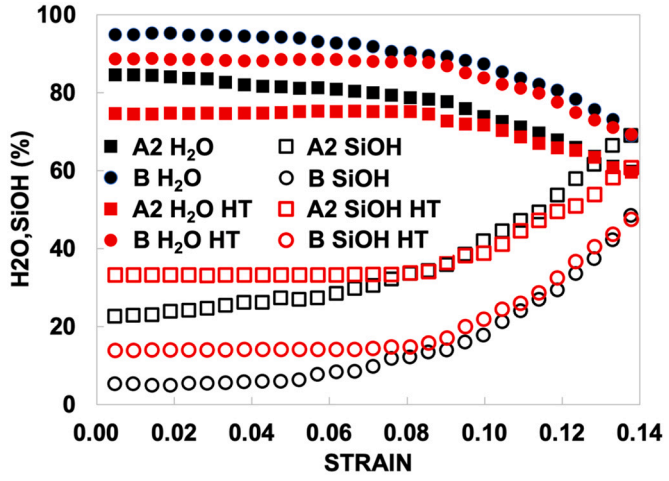

Fig. 5. Changes in H_2O and SiOH concentrations as a percent of the original 5 wt% water added to the A2 and B glasses as a function of strain. HT indicates those glasses that were heated in step 6 of Fig. 1.

that is subsequently stable with increasing strain until the reaching the same strain as the unheated wet systems that show a similar change in slope near the maximum stress seen in Fig. 2.

The increased concentrations of silanols in glass A2 in comparison to glass B is seen to cause a greater compressive stress on the wet glasses that were returned to their initial dimensions (step 4 in Fig. 1). This is consistent with the earlier work that showed that silanols and not water molecules cause expansion of silica [31,34]. Thus, upon return to the initial x dimension, the volume is smaller than expected for the resultant silanol concentration, hence putting the glass into greater compression that results in the greater fracture stress.

4. Conclusions

Molecular dynamics simulations employing a robust reactive interatomic potential of the fracture strength of silica glass samples exposed to water molecules while under tensile stress, with and without heating, followed by return to the original dimension and subsequently strained to failure showed trends consistent with experimentally observed behavior. The fracture behavior of bulk dry glasses was compared to those that had a 5% tensile strain, resulting in a ~ 5–6 GPa stress, followed by random inclusion of 5 wt% water molecules and return to the original dimension via a negative strain. The wet bulk glasses were subsequently strained to failure. Results show that the pre-stressed wet glasses had strength enhancements of ~4–8% in comparison to the original dry glasses. Heating the glasses while pre-stressed with included water, followed by cooling and return to the original size, resulted in an even greater strength enhancement. Of course, the protocols used here can only mimic but not reproduce the experimental procedures, for obvious reasons, but the results are consistent with the innovative experimental data obtained by Tomozawa's group.

The glasses with a higher concentration of structural defects in the dry state have an expected lower dry-glass strength in comparison to a glass with fewer defects. However, the weaker dry glasses showed a greater percentage strength enhancement after water exposure under stress. This is attributed to an increase in the concentration of silanols (SiOH's) in the more defective glass that partially offset the otherwise weakened glass. Increased silanol concentration has previously been shown to increase the expansion of silica glass. This creates an increased compressive stress on the stressed-wet glass relaxed to original dimensions, allowing for an increased strength enhancement.

Declaration of Competing Interest

The authors declare that they have no known competing financial interests or personal relationships that could have appeared to influence the work reported in this paper.

Data availability

Data will be made available on request.

Acknowledgements

The authors acknowledge support from National Science Foundation Enviromental Chemical Science Program of the Division of Chemistry, grant number 1609044.

References

[1] P.J. Lezzi, E.E. Evke, E.M. Aaldenberg, M. Tomozawa, Surface crystallization and water diffusion of silica glass fibers: causes of mechanical strength degradation, J. Am. Ceram. Soc. 98 (2015) 2411–2421.
[2] M. Tomozawa, E.M. Aaldenberg, The role of water in surface stress relaxation of glass, Phys. Chem. Glasses Eur. J. Glass Sci. Technol. B 58 (2017) 154–164.
[3] P.J. Lezzi, Q.R. Xiao, M. Tomozawa, T.A. Blanchet, C.R. Kurkjian, Strength increase of silica glass fibers by surface stress relaxation: a new mechanical strengthening method, J. Non-Cryst. Sol. 379 (2013) 95–106.
[4] P.J. Lezzi, M. Tomozawa, R.W. Hepburn, Confirmation of thin surface residual compressive stress in silica glass by Ftir reflection spectroscopy, J. Non-Cryst. Sol. 390 (2014) 13–18.
[5] M. Tomozawa, D.-L. Kim, A. Agarwal, K.M. Davis, Water diffusion and surface strutural relaxation in silica glasses, J. Non-Cryst. Sol. 288 (2001) 73–80.
[6] M. Tomozawa, P.J. Lezzi, R.W. Hepburn, T.A. Blanchet, D.J. Cherniak, Surface stress relaxation and resulting residual stress in glass fibers: a new mechanical strengthening mechanism of glasses, J. Non-Cryst. Sol. 358 (2012) 2650–2662.
[7] M. Tomozawa, R.W. Hepburn, Surface structural relaxation of silica glass: a possible mechanism of mechanical fatigue, J. Non-Cryst. Sol. 345&346 (2004) 449–460.
[8] P.J. Lezzi, M. Tomozawa, An overview of the strengthening of glass fibers by surface stress relaxation, Int. J. Appl. Glas. Sci. 6 (2015) 34–44.
[9] S.M. Wiederhorn, T. Fett, G. Rizzi, M.J. Hoffmann, J.-P. Guin, Water penetration—its effect on the strength and toughness of silica glass, Met. Matl. Trans. A (2013) 1164–1174.
[10] J. Sauer, K.P. Schroder, Geminal hydroxyls on silica surfaces and their role in water adsorption, Z. Phys. Chem. Leipzig 266 (1985) 379–387.
[11] B.C. Bunker, D.M. Haaland, T.A. Michalske, W.L. Smith, Kinetics of dissociative chemisorption on strained edge-shared surface defects on dehydroxylated silica, Surf. Sci. 222 (1989) 95–118.
[12] T. Michalske, S. Freiman, A molecular interpretation of stress corrosion in silica, Nature 295 (1982) 511–512.
[13] T.A. Michalske, B.C. Bunker, Slow fracture model based on strained silicate structures, J. Appl. Phys. 56 (1984) 2686–2693.
[14] C.J. Brinker, R.K. Brow, D.R. Tallant, R.J. Kirkpatrick, Surface structure and chemistry of high surface area silica gels, J. Non-Cryst. Solids 120 (1990) 26–33.
[15] B.P. Feuston, S.H. Garofalini, Water-induced relaxation of the vitreous silica surface, J. Appl. Phys. 68 (1990) 4830–4836.
[16] Y. Xiao, A.C. Lasaga, Ab initio quantum mechanical studies of the kinetics and mechanisms of silicate dissolution: H+(H3o+) catalysis, Geochim. Cosmochim. Acta 58 (1994) 5379–5400.
[17] A. Pelmenschikov, H. Strandh, L.G.M. Pettersson, J. Leszczynski, Lattice resistance to hydrolysis of Si-O-Si bonds of silicate minerals: ab initio calculations of a single water attack onto the (001) and (111) beta-cristobalite surfaces, J. Phys. Chem. B 104 (2000) 5779–5783.
[18] Y. Ma, A.S. Foster, R.M. Nieminen, Reactions and clustering of water with silica surface, J. Chem. Phys. 122 (2005).
[19] J.C. Du, A.N. Cormack, Molecular dynamics simulation of the structure and hydroxylation of silica glass surfaces, J. Am. Ceram. Soc. 88 (2005).
[20] S.H. Garofalini, T.S. Mahadevan, S. Xu, G.W. Scherer, Molecular mechanisms causing anomalously high thermal expansion of nanoconfined water, ChemPhysChem 9 (2008) 1997–2001.
[21] T.S. Mahadevan, S.H. Garofalini, Dissociative chemisorption of water onto silica surfaces and formation of hydronium ions, J. Phys. Chem. C 112 (2008) 1507–1515.
[22] G.K. Lockwood, S.H. Garofalini, Bridging oxygen as a site for proton adsorption on the vitreous silica surface, J. Chem. Phys. 131 (2009), 074703.
[23] S. Xu, G.W. Scherer, T.S. Mahadevan, S.H. Garofalini, Thermal expansion of confined water, Langmuir 25 (2009) 5076–5083.
[24] D.K. Murray, Differentiating and characterizing geminal silanols in silicas by 29si Nmr spectroscopy, J. Colloid Interface Sci. 352 (2010) 163–170.
[25] I.C. Bourg, C.I. Steefel, Molecular dynamics simulations of water structure and diffusion in silica nanopores, J. Phys. Chem. C 116 (2012) 11556–11564.
[26] M. Kagan, G.K. Lockwood, S.H. Garofalini, Reactive simulations of the activation barrier to dissolution of amorphous silica in water, Phys. Chem. Chem. Phys. 16 (2014) 9294–9301.
[27] G.K. Lockwood, S.H. Garofalini, Proton dynamics at the water-silica interface via dissociative molecular dynamics, J. Phys. Chem. C 118 (2014) 29750–29759.
[28] K. Leung, I.M.B. Nielsen, L.J. Criscenti, Elucidating the bimodal acid-base behavior of the water-silica interface from first principles, J. Am. Chem. Soc. 131 (2009) 18358–18365.
[29] F. Musso, P. Mignon, P. Ugliengo, M. Sodupe, Cooperative effects at water-crystalline silica interfaces strengthen surface silanol hydrogen bonding. An ab initio molecular dynamics study, Phys. Chem. Chem. Phys. 14 (2012) 10507–10514.
[30] J. Du, J.M. Rimza, Atomistic computer simulations of water interactions and dissolution of inorganic glasses, npj Mat. Deg. 16 (2017) 1–12.
[31] S.H. Garofalini, J. Lentz, M. Homann, Molecular mechanism of the expansion of silica glass upon exposure to moisture, J. Am. Ceram. Soc. 103 (2020) 2421–2431.
[32] M. Gierada, F. De Proft, M. Sulpizi, F. Tielens, Undertanding the acidic properties of the amorphous hydroxylated silica surface, J. Phys. Chem. C 123 (2019) 17343–17352.
[33] M. Sulpizi, M.-P. Gaigeot, M. Sprik, The silica-water interface: how the silanols determine the surface acidity and modulate the water properties, J. Chem. Theory Comput. 8 (2012) 1037–1047.
[34] S.M. Wiederhorn, F. Yi, D. LaVan, L.J. Richter, T. Fett, M.J. Hoffmann, Volume expansion caused by water penetration into silica glass, J. Am. Ceram. Soc. 98 (2015) 78–87.
[35] T. Fett, K.G. Schell, M.J. Hoffmann, S.M. Wiederhorn, Effect of damage by hydroxyl generation on strength of silica fibers, J. Am. Ceram. Soc. 101 (2018) 2724–2726.

[36] S.M. Wiederhorn, T. Fett, G. Rizzi, S. Fünfschilling, M.J. Hoffmann, J.-P. Guin, Effect of water penetration on the strength and toughness of silica glass, J. Am. Ceram. Soc. 94 (2011) s196–s203.
[37] S. Wiederhorn, A chemical interpretation of static fatigue, J. Am. Ceram. Soc. 55 (1971) 81–85.
[38] J.E. Shelby, Density of vitreous silica, J. Non-Cryst. Sol. 349 (2004) 331–336.
[39] R. Bruckner, The structure-modifying influence of the hydroxyl content of vitreous silicas, Glastech. Ber. 43 (1970) 8–12.
[40] T.S. Mahadevan, S.H. Garofalini, Dissociative water potential for molecular dynamics simulations, J. Phys. Chem. B 111 (2007) 8919–8927.
[41] J. Lentz, S.H. Garofalini, Structural aspects of the topological model of the hydrogen bond in water on auto-dissociation via proton transfer, Phys. Chem. Chem. Phys. 20 (2018) 16414–16427.
[42] G.K. Lockwood, S.H. Garofalini, Lifetimes of excess protons in water using a dissociative water potential, J. Phys. Chem. B 117 (2013) 4089–4097.
[43] D. Marx, M.E. Tuckerman, M. Parrinello, Solvated excess protons in water: quantum effects on the hydration structure, J. Phys. Condens. Matter 12 (2000) A153–A159.
[44] J. Lentz, S.H. Garofalini, Vibrational dynamics of the od stretch in an atomistic simulation of HDO in H_2O, J. Mol. Liq. (2022) 367.
[45] J. Lentz, S.H. Garofalini, Role of the hydrogen bond lifetimes and rotations at the water/amorphous silica interface on proton transport, Phys. Chem. Chem. Phys. 21 (2019) 12265–12278.
[46] S.K. Park, K.W. Miller, Random Numner generators: good ones are hard to find, Commun. ACM 31 (1988) 1192–1201.
[47] C. Bays, S.D. Durham, Improving a poor random number generator, ACM Trans. Math. Softw. 2 (1976) 59–64.
[48] E.B. Webb, S.H. Garofalini, Molecular dynamics simulation of the approach and withdrawal of a model crystalline metal to a silica glass surface, J. Chem. Phys. 101 (1994) 10101–10106.
[49] O.R. Walton, Discussion: stress and strain analysis in molecular dynamics simulation of solids, J. Appl. Mech. 64 (1997) 247.